

See discussions, stats, and author profiles for this publication at: <https://www.researchgate.net/publication/244286652>

# Study of hydrogen bond polarized IR spectra of cinnamic acid crystals

ARTICLE *in* JOURNAL OF MOLECULAR STRUCTURE · NOVEMBER 2004

Impact Factor: 1.6 · DOI: 10.1016/j.molstruc.2004.06.032

CITATIONS

34

READS

162

## 2 AUTHORS:



[Henryk T Flakus](#)

University of Silesia in Katowice

96 PUBLICATIONS 1,175 CITATIONS

[SEE PROFILE](#)



[Magdalena Jabłońska-Czapla](#)

Polish Academy of Sciences

74 PUBLICATIONS 345 CITATIONS

[SEE PROFILE](#)

# Study of hydrogen bond polarized IR spectra of cinnamic acid crystals

Henryk T. Flakus\*, Magdalena Jabłońska

*Institute of Chemistry, University of Silesia, 9 Szkolna Street, PL-40-006 Katowice, Poland*

Received 9 March 2004; revised 14 June 2004; accepted 22 June 2004

Available online 19 August 2004

## Abstract

This paper presents the results of investigation of the polarized IR spectra of cinnamic acid and of its deuterium derivative crystals. The spectra were measured by a transmission method, using polarized light, at the room temperature and at 77 K, for two different crystalline faces. Theoretical analysis of the results concerned linear dichroic effects, H/D isotopic and temperature effects, observed in the spectra of the hydrogen and of the deuterium bonds in cinnamic acid crystals, at the frequency ranges of the  $\nu_{\text{O-H}}$  and the  $\nu_{\text{O-D}}$  bands. The basic crystal spectral properties could be satisfactorily interpreted in a quantitative way for a centrosymmetric cyclic hydrogen bond dimer model. Such a model explains not only a two-branch structure of the  $\nu_{\text{O-H}}$  and  $\nu_{\text{O-D}}$  bands in crystalline spectra, but also some essential linear dichroic effects in the band frequency ranges, measured for isotopically diluted crystals. Model calculations, performed within the limits of the ‘strong-coupling’ model, allowed for quantitative interpretation and for understanding of the basic properties of the hydrogen bond IR spectra of cinnamic acid crystals, H/D isotopic, temperature and dichroic effects included. In the scope of our studies the mechanism of H/D isotopic ‘self-organization’ processes, taking place in the crystal hydrogen bond lattices, was also recognized. It was proved that for isotopically diluted crystalline samples of cinnamic acid, a non-random distribution of protons and deuterons occurs exclusively in the hydrogen bond dimers. Nevertheless, these co-operative interactions between the hydrogen bonds do not involve the adjacent hydrogen bond dimers in each unit cell. The two-branch fine structure pattern of the  $\nu_{\text{O-H}}$  and  $\nu_{\text{O-D}}$  bands was ascribed to the vibronic mechanism of vibrational dipole selection rule breaking in centrosymmetric hydrogen bond dimers. The observed in the spectra very high intensity of the forbidden transition sub-band in the analyzed  $\nu_{\text{O-H}}$  and  $\nu_{\text{O-D}}$  bands is a manifestation of an extremely effective symmetry rule breaking mechanism. It correlates with a relatively large excess electron charge on the cinnamic acid dimer carboxyl groups. This effect is a result of a partial withdrawal of the electron charge, from the conjugated  $\pi$ -bond systems of the styryl substituents, by the carboxyl groups. This statement has been supported by *ab initio* calculations.

© 2004 Elsevier B.V. All rights reserved.

**Keywords:** Hydrogen bond; Molecular crystals; Polarized IR spectra; H/D isotopic effects; Linear dichroic effects; Temperature effects; Model calculations; Isotopic dilution; H/D isotopic ‘self-organization’ effects

## 1. Introduction

Infrared spectroscopy is still considered a powerful tool in the area of the hydrogen bond research. The subject of a particular interest of researchers are the spectral properties of the  $\nu_{\text{X-H}}$  bands in the IR, connected with excitation of the proton stretching vibrations in the  $\text{X-H}\cdots\text{Y}$  hydrogen bridges. The hydrogen bond formation in molecular systems is responsible for a strong increase of the  $\nu_{\text{X-H}}$  band integral intensities, a considerable decrease of the band frequencies and their considerable widening, when compared with

the corresponding band parameters for the non-associated X–H group spectra. Intensive studies on hydrogen bond IR spectra concerned not only the frequencies of vibrational transitions in these band frequency ranges, the band integral intensities and the bandwidths, but also some basic H/D isotopic effects in the spectra [1–5]. A particular interest of the researchers was focussed on the fine structure pattern of the  $\nu_{\text{X-H}}$  bands. This latest property has been considered as a result of strong dynamic anharmonic couplings between the hydrogen bond vibrations, involving the atoms participating in forming of the hydrogen bridges [2–5]. Theoretical models, the earlier qualitative and the latest quantitative ones, elaborated during the recent 50 years, tried to explain the basic spectral properties of hydrogen bond systems

\* Corresponding author. Fax: +48-32-2599-978.

E-mail address: [flakus@ich.us.edu.pl](mailto:flakus@ich.us.edu.pl) (H.T. Flakus).

[1–5]. The quantitative models considered advanced coupling mechanisms, involving the hydrogen bond normal vibrations, which in a consequence allowed numerical reconstitution of theoretical  $\nu_{X-H}$  bands. Also spectra of some deuterium-bonded systems, measured in the  $\nu_{X-D}$  band frequency ranges, were theoretically reproduced. These quantitative theoretical models belong to so-called ‘strong-coupling’ theory [6–8], the elder, and to the latest more general theoretical model, so-called ‘relaxation’ theory [9–12]. The both theoretical models have seen the source of generation of the hydrogen bond spectra in purely vibrational mechanisms.

The ‘strong-coupling’ theory succeeded in a quantitative description of IR spectra of single, isolated hydrogen bond systems, but also of simple aggregates of hydrogen bonds, including hydrogen bond dimers [6,7]. This model was also successfully applied for quantitative interpretation of the IR spectra of hydrogen-bonded molecular crystals [13–19].

Latest experimental data, obtained by measuring polarized spectra of hydrogen-bonded molecular crystals have proved that the spectra generation mechanism was in a high degree of an electronic nature. Polarized IR spectra, measured for spatially oriented monocrystalline layers, can provide a most complete information about vibrational transition moment directions, for systems of mutually interacting hydrogen bonds, about the energies of exciton states and about the degree of complexity of the  $\nu_{X-H}$  bands. Recent investigation of the polarized spectra of hydrogen-bonded molecular crystal allowed revealing a number of new and non-conventional spectral effects. Explanation of these effects appeared impossible when based on a purely vibrational approach. To these new effects belongs the breaking of the vibrational dipole selection rules, in the IR for centrosymmetric hydrogen bond dimers [20]. This effect is a unique attribute of centrosymmetric hydrogen bond dimers, while isolated centrosymmetric molecules exhibit regular vibrational selection rules in the IR. The classical literature on the IR spectroscopy never considered such spectral phenomena.

Another, non-conventional spectral behavior, revealed for hydrogen-bonded crystals, concerned H/D isotopic effects of the hydrogen bond. To this group of effect belongs so-called ‘long-range’ isotopic effects [21], as well as so-called H/D ‘self-organization’ isotopic effects in hydrogen bond systems, depending on a non-random distribution of protons and deuterons between the hydrogen bonds of crystalline lattices [22–24]. All these newly described effects were explained by strong vibronic coupling mechanisms, in the lattices of hydrogen-bonded crystals [25]. However, they need further intensive studies, also utilizing the IR spectroscopy in polarized light, applied for suitable model solid-state systems.

The problem of vibrational dipole selection rule breaking in the IR, for centrosymmetric hydrogen bond dimers, seems to be of a particular interest. In studies of the hydrogen bond spectral properties, the O–H $\cdots$ O hydrogen

bond dimers, formed by associated carboxylic acid molecules, were many times the object of analyzes as proper model systems. The spectra of carboxylic acid crystals were confronted with the subsequently developed theoretical models. Carboxylic acid molecules form dimers not only in the gaseous phase, but also in the lattices of carboxylic acid crystals (The only exception are the formic acid and acetic acid crystals). Although in each case the hydrogen bond dimers, formed by the associated carboxyl groups (COOH)<sub>2</sub> are fairly identical, the  $\nu_{O-H}$  bands differ with regard to the fine structure pattern and to the intensity distribution. Explaining these phenomena seems essential for understanding of the nature of the hydrogen bond IR spectra generation mechanisms, vibronic coupling mechanisms, involving electronic motions and the normal vibrations in hydrogen bond dimers.

The observed differences between the spectral properties of different carboxylic acid crystals should be intuitively connected with the electronic structure of hydrogen-bonded carboxylic acid molecules. During systematic spectral studies noticeable differences between spectra of aliphatic carboxylic acid crystals [26,27], aryl carboxyl acid [28] and arylaliphatic carboxyl acid crystals [29] were observed. In the case of benzoic acid crystals [27] and of 1-naphthoic acid and 2-naphthoic acid crystals [30], the vibrational selection rule breaking effects were extremely strong for the  $\nu_{O-H}$  band frequency range. This statement can be supported by a very high relative intensity of the longer-wave  $\nu_{O-H}$  band branch in each of the crystal IR spectra. According to the theory [20], the band branch intensity was basically determined by the vibronically activated forbidden transition.

A quite different spectral behavior is characteristic for hydrogen-bonded phenylacetic acid [29] and for 1-naphthylacetic and 2-naphthylacetic acid crystals [31]. In the crystalline spectra, the longer-wave branch of each  $\nu_{O-H}$  band was of an extremely low intensity. This fact seems prove that for these systems the forbidden transition mechanism is non-effective enough, due to separation of the vibrating protons in the hydrogen bonds from the  $\pi$ -electron systems by methylene groups. Therefore, the vibronic promotion mechanism, which according to the theoretical model [20], is the source of the selection rule breaking, most probably become weakened.

The hypothesis presented above, concerning the vibronic nature of the forbidden transition activation mechanism could be verified by investigation of spectral properties of a model carboxylic acid crystal, for which the carboxyl groups in the molecules are being separated from aromatic rings by a C=C double bond. Cinnamic acid is a compound with its molecules satisfying these demands. In the cinnamic acid molecules the carboxyl groups are linked with styryl substituents and, therefore, they couple with the extended delocalized  $\pi$ -electronic systems. One might expect relatively strong selection rule breaking effects, in the spectra of cinnamic acid crystals, in the frequency range of the  $\nu_{O-H}$

band. Therefore, the hydrogen bond spectra of cinnamic acid crystals in some aspects should rather resemble the benzoic acid crystal spectrum, than the spectrum of phenylacetic acid crystals. The expected spectral behavior of cinnamic acid crystals would provide strong arguments, supporting the vibronic model for activation of the forbidden vibrational transition, in centrosymmetric hydrogen bond dimers.

This paper presents the investigation results of the polarized IR spectra of cinnamic acid crystals. The aim of this work was to illuminate the nature of the generation mechanisms of the hydrogen bond dimer IR spectra. The analysis of the forbidden transition breaking mechanisms demanded a quantitative interpretation of the cinnamic acid crystal polarized IR spectra and also of the polarized spectra of isotopically diluted cinnamic acid crystals.

## 2. Crystallographic structure of cinnamic acid

The X-ray structure of trans-cinnamic acid crystals was determined recently by Bryan and Freyberg [32]. The crystal is monoclinic, space symmetry group is  $P2_1/n$ ,  $Z=4$ . In a unit cell there are two centrosymmetric dimers, linked by two O–H...O hydrogen bonds. The unit cell parameters are:  $a=5.644(1)$  Å,  $b=18.011(6)$  Å,  $c=9.019(3)$  Å and  $\beta=121.47(2)^\circ$ . Cinnamic acid crystals usually develop the 'ac' or the 'bc' crystalline face.

## 3. Experimental

Cinnamic acid ( $C_6H_5-CH=CH-COOH$ ) used for our studies was the commercial substance (Sigma-Aldrich). For our studies it was used without further purification.

Crystals suitable for the spectral studies were obtained by crystallization from melt, between two closely spaced  $CaF_2$  windows. In this way sufficiently thin crystals (grey in transparent light) could be obtained, characterized by their maximum absorbance at the  $\nu_{O-H}$  band frequency range being close to 0.5. From the crystal mosaic, suitable monocrystalline fragments were selected and then spatially oriented, with the help of a polarization microscope. It was found that most frequently the crystals developed the 'bc', or the 'ac' crystalline faces. These crystals were exposed for the experiment by use of a tin diaphragm with a 1.5 mm hole diameter. For each crystal face case, 'bc' and 'ac', at least 8 single crystals were investigated. The IR spectra were measured at the room temperature and at the temperature of liquid nitrogen, using polarized radiation, with two different orientations of the electric field vector ' $E$ ', with respect to the crystal lattice. All the spectra were measured by a transmission method at  $2\text{ cm}^{-1}$  resolution. In a similar way measurements of spectra were performed for cinnamic acid deuterium derivative crystals, which were synthesized by evaporation of the compound solution in  $D_2O$  under reduced

pressure. We measured spectra of ca. 15 single crystals of cinnamic acid, representing the both crystal face cases, 'bc' and 'ac'. The deuterium substitution rate for individual crystals investigated varied in a relatively wide range (from 50 to 90%).

The Raman spectra were measured at the room temperature for polycrystalline samples of cinnamic acid, using the Raman Accessory for the Nicolet Magna 560 spectrometer.

## 4. Results

### 4.1. Initial studies

The initial experimental studies consisted in measuring of the cinnamic acid IR spectra for the  $CCl_4$  solution and for polycrystalline samples of the compound, dispersed in KBr pellets. In Fig. 1 the  $CCl_4$  solution spectra of cinnamic acid are being presented, measured in the frequency ranges of the  $\nu_{O-H}$  and of the  $\nu_{O-D}$  bands.

Spectra of polycrystalline samples of cinnamic acid, measured in the same frequency ranges at two different

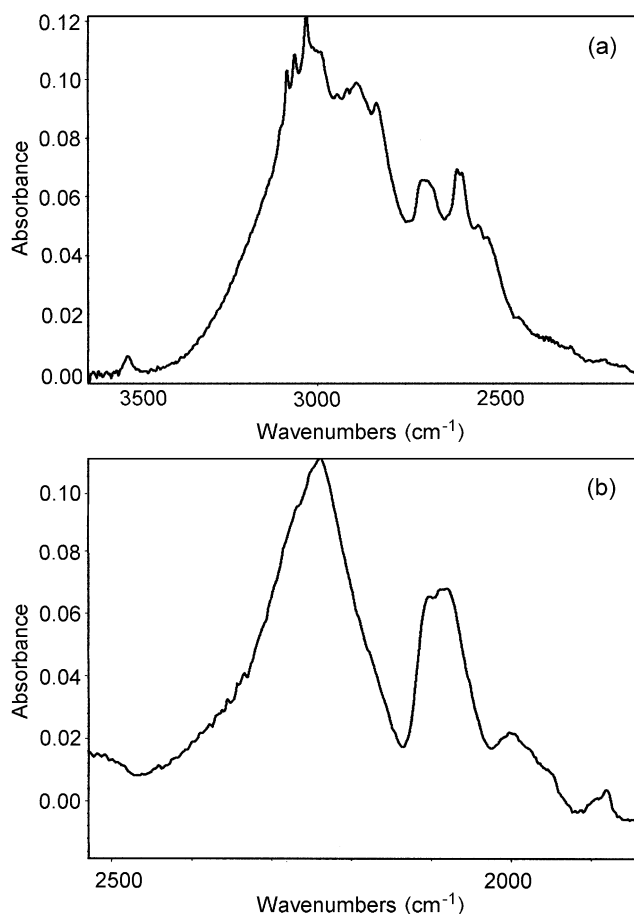


Fig. 1. The IR spectra of cinnamic acid in the  $CCl_4$  solution. (a) The  $\nu_{O-H}$  band. (b) The  $\nu_{O-D}$  band.

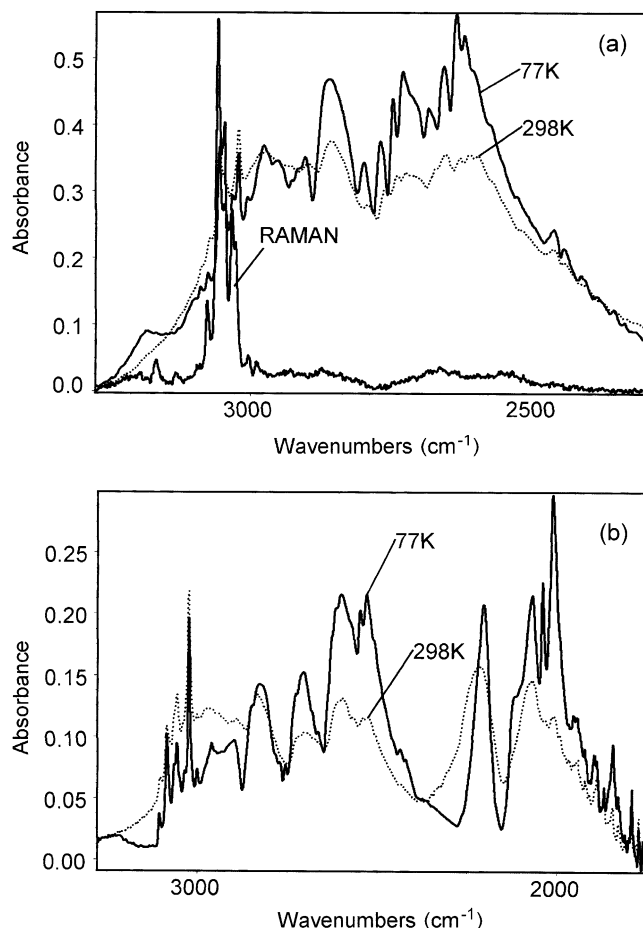


Fig. 2. The IR spectra of the polycrystalline samples of cinnamic acid, dispersed in KBr pellets, measured at 298 and 77 K. (a) The  $\nu_{\text{O-H}}$  band. The Raman spectrum of the polycrystalline samples is also being drawn in order to indicate the  $\nu_{\text{C-H}}$  band influence on the spectra. (b) The  $\nu_{\text{O-D}}$  band.

temperatures, by use of the KBr pellet techniques, are shown in Fig. 2.

For cinnamic acid molecules a relatively wealthy spectrum of  $\nu_{\text{C-H}}$  bands may be expected. These narrow bands might influence the  $\nu_{\text{O-H}}$  band contour. Identification of these bands is possible, when based on Raman spectra, where the  $\nu_{\text{C-H}}$  bands are characterized by considerably higher intensities, when compared with the  $\nu_{\text{O-H}}$  band intensities. The Raman spectrum of cinnamic acid polycrystalline sample is also drawn in Fig. 2. These results show that the  $\nu_{\text{C-H}}$  bands only slightly deform the  $\nu_{\text{O-H}}$  band contour.

For the  $\text{CCl}_4$  solution spectrum, the shorter-wave branch of the  $\nu_{\text{O-H}}$  band (i.e. appearing at ca.  $3000\text{ cm}^{-1}$ ) is more intense, when compared with the longer-wave band branch (at  $2700\text{ cm}^{-1}$ ). For the solid-state spectra, measured for KBr pellets, this relation is more complicated, as a relatively strong influence of temperature on the intensity distribution in the  $\nu_{\text{O-H}}$  band can be observed. Diminution of temperature, from 298 to 77 K, causes a considerable increase of the  $\nu_{\text{O-H}}$  band longer-wave branch intensity. Qualitatively similar behavior also concerns the  $\nu_{\text{O-D}}$  band, which also exhibits a two-branch fine structure pattern.

#### 4.2. Polarized spectra of cinnamic acid crystal

Polarized spectra of cinnamic acid crystals, measured at the room temperature, in the frequency range of the  $\nu_{\text{O-H}}$  and  $\nu_{\text{C-H}}$  bands, for the two crystalline faces, 'ac' and 'bc', are shown in Fig. 3a and b.

The  $\nu_{\text{O-H}}$  bands are characterized by a wealthy fine structure pattern, in the both spectral branches. A considerable change in the band contour shapes of the  $\nu_{\text{O-H}}$  band polarized components can be observed, when comparing the spectra recorded for the two different crystal planes. The polarized spectra exhibit two kinds of polarization effects: The main polarization effect in the spectra simply results from geometrical factors, i.e. from the orientation of the electric field vector 'E', with respect to the crystal lattice, in the experimental conditions (The effects of the 'first kind'). Other polarization effects in the spectra result from relatively strong *Davydov couplings*, influencing the  $\nu_{\text{O-H}}$  band polarized components.

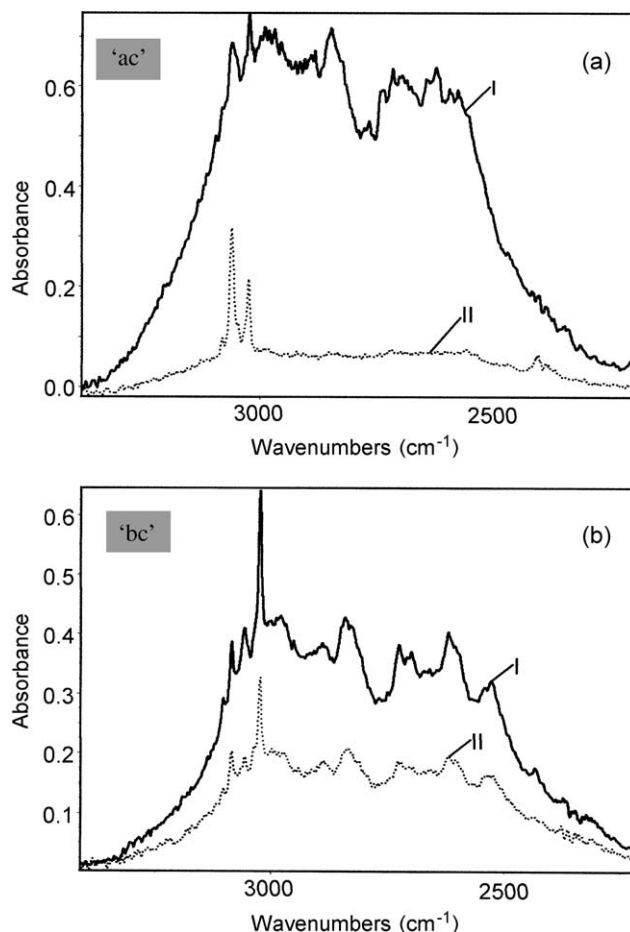


Fig. 3. Polarized IR spectra of cinnamic acid single crystals, measured at the room temperature in the  $\nu_{\text{O-H}}$  and the  $\nu_{\text{C-H}}$  band frequency range. The IR beam of normal incidence with respect to the different crystal faces, 'ac' and 'bc', was applied. In each case the component spectra were obtained for two orientations of the electric field vector *E*. (a) The 'ac' plane, (I)  $E\parallel c$ , (II)  $E\perp c$  ( $E\parallel a^*$ ). (b) The 'bc' plane, (I)  $E\parallel c$ , (II)  $E\perp c$  ( $E\parallel b$ ). The  $a^*$  symbol denotes the vector in the reciprocal lattice. Spectra (I) and (II) were drawn on a common scale.



These latest effects seem to be the main source of the observed differences in the polarized band shapes, corresponding to the two different crystalline faces (The effects of the ‘second kind’).

The low-temperature polarized spectra of the same cinnamic acid crystals, measured at 77 K in the same frequency range, are presented in Fig. 4a and b.

Diminution of temperature enhances the observed difference between the spectra, obtained for the two different crystalline faces. Nevertheless, no substantial changes are being noticed for the strongest polarization effects in the spectra, which relate to the geometrical factors of the spectral experiments. The polarization effects of the ‘second kind’ seem indicate a role of relatively strong *Davydov-splitting* effects, in generation of the fine structure patterns of the  $\nu_{\text{O-H}}$  bands, in the cinnamic acid crystal spectra. The cinnamic acid crystal spectral properties seem to be extreme ones, in comparison with the corresponding spectral properties of another carboxylic acid crystals [27,33], whose spectra can be satisfactorily interpreted in terms of the ‘oriented-gas’ model. This model gas would be composed with centrosymmetric cyclic dimers of the  $\text{O-H}\cdots\text{O}$  hydrogen bonds, formed in the associated carboxyl groups  $(\text{COOH})_2$ .

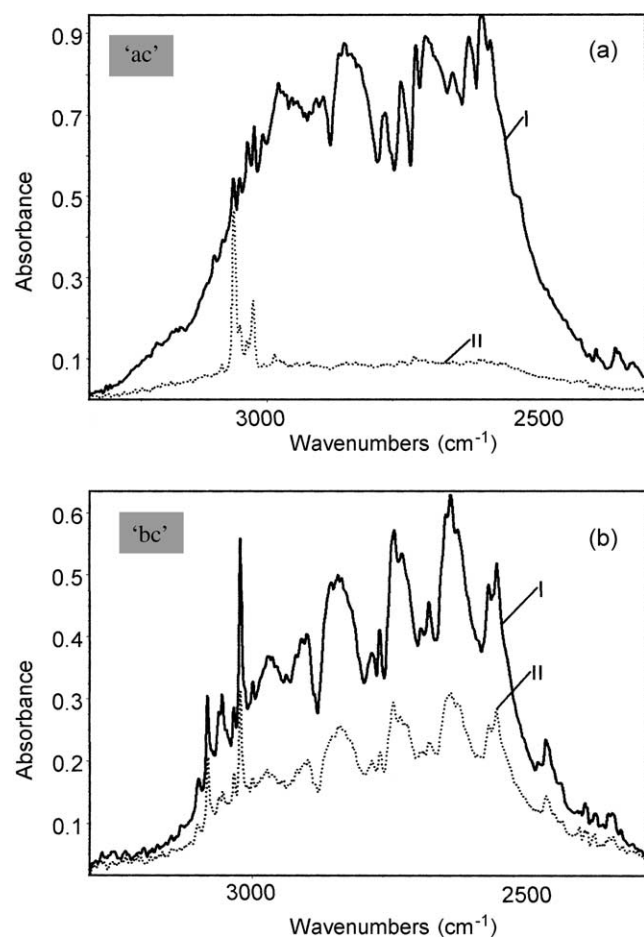


Fig. 4. Polarized IR spectra of cinnamic acid single crystals, measured at 77 K in the  $\nu_{\text{O-H}}$  and the  $\nu_{\text{C-H}}$  band frequency range. Other experimental conditions and the way of presentation is identical with those given in Fig. 3.

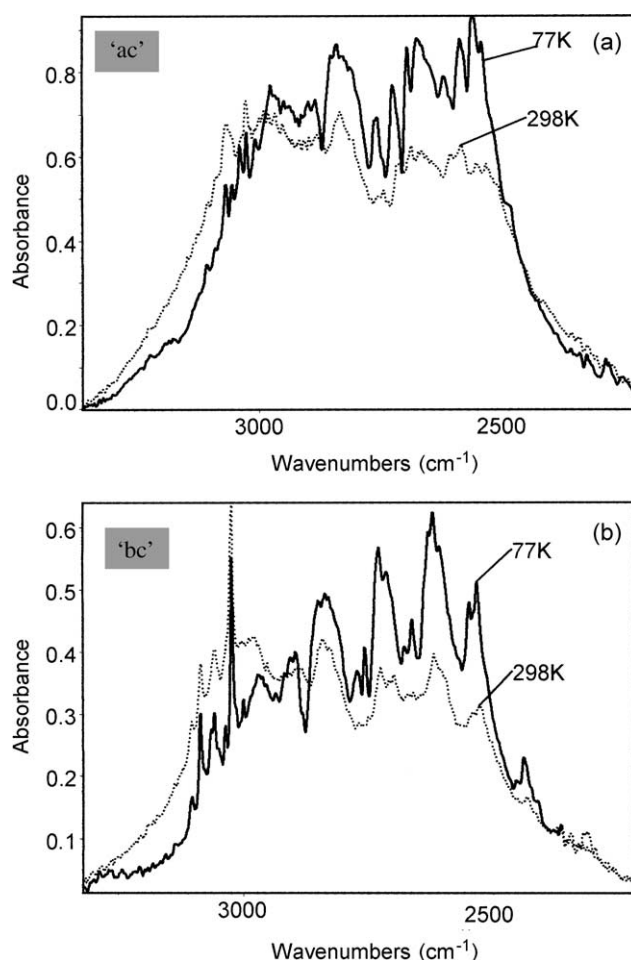


Fig. 5. The impact of temperature on the most intense polarized component  $\nu_{\text{O-H}}$  band contours in the IR spectra of cinnamic acid crystals. (a) The ‘ac’ plane, (b) The ‘bc’ plane.

When temperature decreases, a noticeable change in the  $\nu_{\text{O-H}}$  band shapes occurs. At the room temperature the longer-wave branch of the band is characterized by a lower intensity, when compared with the shorter-wave branch. Diminution in temperature is responsible for a relatively strong intensity growth of the longer-wave branch of the  $\nu_{\text{O-H}}$  band polarized components. Fig. 5a and b shows the temperature induced evolution of the most intense polarized components of the  $\nu_{\text{O-H}}$  bands, from the cinnamic acid crystal spectra, measured for both different crystal planes, ‘ac’ and ‘bc’.

#### 4.3. Polarized spectra of D-cinnamic acid crystals

Polarized IR spectra of cinnamic acid crystals, characterized by relatively high substitution rates of deuterons in the hydrogen bridges, measured at the room temperature, are shown in Fig. 6a and b. These spectra were measured in a more extended frequency range, covering the  $\nu_{\text{O-D}}$ , as well as the ‘residual’  $\nu_{\text{O-H}}$  bands, for crystals having developed one from the following crystalline faces, ‘ac’ or ‘bc’. At this point it must be emphasized, that the measured  $\nu_{\text{O-D}}$  bands

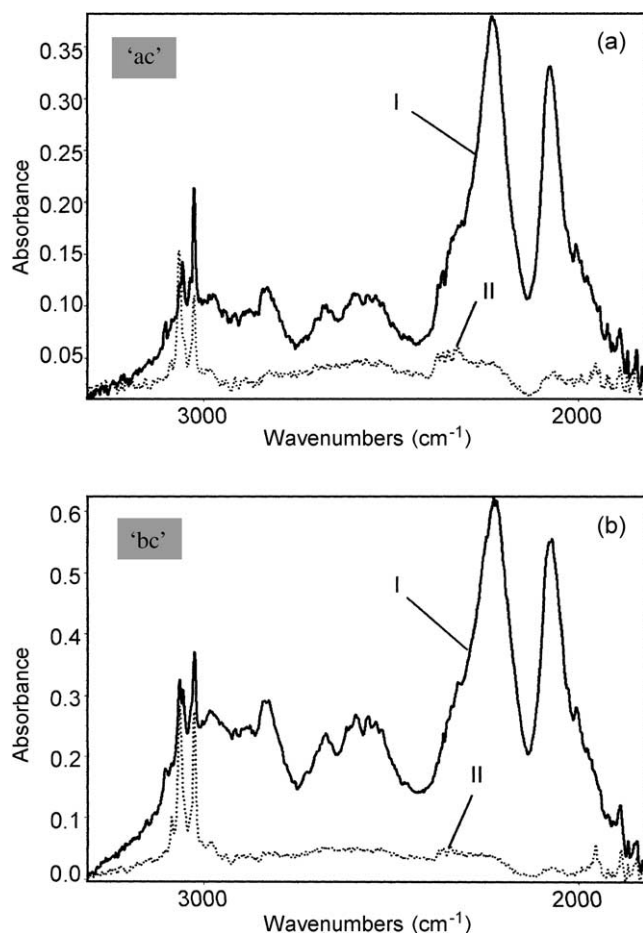


Fig. 6. Polarized IR spectra of isotopically diluted with deuterium cinnamic acid single crystals, measured at the room temperature in the  $\nu_{\text{O-D}}$  and the 'residual'  $\nu_{\text{O-H}}$  band frequency ranges. (a) The 'ac' plane, 80% D, 20% H, (b) The 'bc' plane, 65% D, 35% H. Other experimental conditions and the way of presentation is identical with those given in Fig. 3.

are the attribute of crystals with a mixed content of deuterons and protons in the crystal hydrogen bridges. Therefore, the  $\nu_{\text{O-D}}$  bands also exhibit a partial character of 'residual' bands.

The low-temperature spectra of the same crystals are being presented in Fig. 7a and b.

As the  $\nu_{\text{O-D}}$  band shapes in the polarized spectra of crystals, having developed different crystalline faces were very similar, the corresponding crystal faces, 'ac' or 'bc', were identified, when based on the spectral band properties, related to a more extended frequency range. In the crystal plane identification procedure, the  $\nu_{\text{C=O}}$  carbonyl group stretching vibration band dichroic properties were analyzed. For the two crystal planes these properties appeared essentially different.

The impact of temperature, on the most intense components of the polarized spectra of isotopically diluted cinnamic acid crystals, is being shown in Fig. 8a and b.

The  $\nu_{\text{O-D}}$  bands exhibit qualitatively similar polarization effects of the 'first kind' like the  $\nu_{\text{O-H}}$  bands, from the spectra of isotopically non-diluted crystals (Figs. 3 and 4).

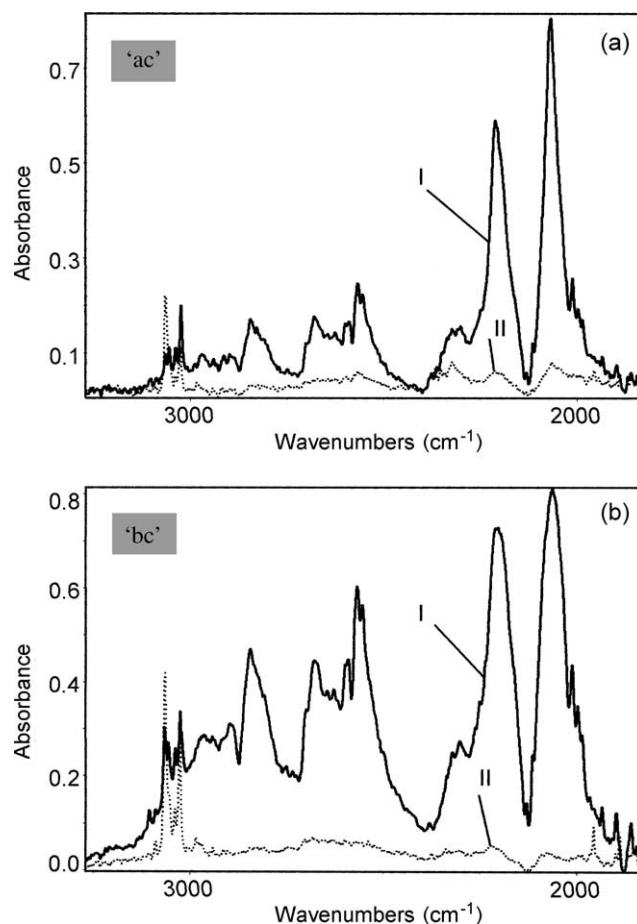


Fig. 7. Polarized IR spectra of isotopically diluted with deuterium cinnamic acid single crystals, measured at 77 K in the  $\nu_{\text{O-D}}$  and the 'residual'  $\nu_{\text{O-H}}$  band frequency ranges. Other experimental conditions and the way of presentation is identical with those given in Fig. 6.

These  $\nu_{\text{O-D}}$  bands, composed with two intense lines only, are narrower and also exhibiting a two-branch fine structure pattern, with temperature-induced evolution similar to the  $\nu_{\text{O-H}}$  band temperature effects. It means that the intensity of the longer-wave branch of these bands also increases with diminution of temperature. However, no essential differences between the  $\nu_{\text{O-D}}$  band shapes, measured for the different crystalline faces, could be noticed. It seemed, however, that these bands still remained complex, although some of *Davydov-splitting* effects were absent in the spectra of D-bonded cinnamic acid crystals.

The measured spectra, in the frequency range of the 'residual'  $\nu_{\text{O-H}}$  bands, also exhibit similar polarization effects of the 'first kind' like the  $\nu_{\text{O-H}}$  bands, of the isotopically 'pure' cinnamic acid crystals (see Fig. 5a and b). Although, the shapes of the 'residual'  $\nu_{\text{O-H}}$  bands were almost independent from the developed crystal plane, the impact of temperature on the spectra was still being observed. It differentiates the spectral properties of the longer-wave branch of the 'residual'  $\nu_{\text{O-H}}$  bands, with respect to the shorter-wave branch properties. These facts indicated that the band fine structure remained still complex,

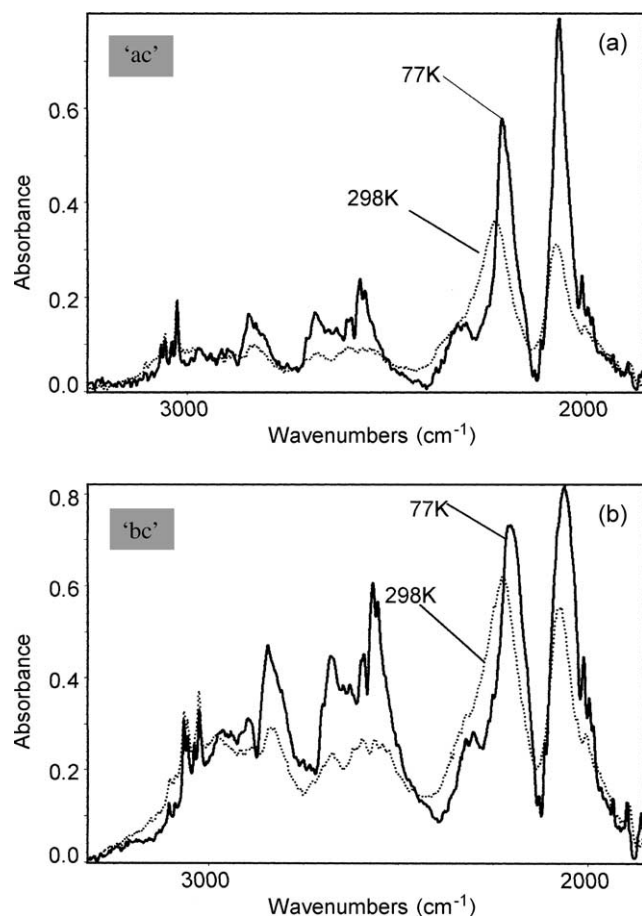


Fig. 8. The impact of temperature on the most intense polarized component  $\nu_{\text{O-D}}$  and the 'residual'  $\nu_{\text{O-H}}$  band contours in the IR spectra of cinnamic acid crystals. (a) The 'ac' plane, 80% D, 20% H, (b) The 'bc' plane, 65% D, 35% H.

despite of isotopic dilution, which was responsible for annihilation of only selected exciton couplings, between the hydrogen bonds in cinnamic acid crystals and in the consequence, for disappearance from the spectra of some Davydov-splitting effects.

## 5. Discussion

The solid-state IR spectra of cinnamic acid exhibited some properties, which demand a deeper understanding. A quantitative description of the spectra seems extremely important for developing the general theory of the hydrogen bond IR spectra of molecular crystals. Polarized spectra could provide a most complete experimental data about the generation mechanisms of hydrogen-bonded system IR spectra. In this way they could extend our knowledge about the hydrogen bond, as a natural phenomenon. In our consideration we will focus on the analysis of the two-branch structure of the  $\nu_{\text{O-H}}$  and the  $\nu_{\text{O-D}}$  bands, with the longer-wave branch of each band having an extremely high intensity. We will also analyze the polarization and the temperature effects in the spectra, isotopic dilution effects in

the crystal spectra and hypothetical *Fermi resonance* effects in the  $\nu_{\text{O-H}}$  bands. Our considerations will be supported by model calculations, aiming to numerically reconstitute the basic properties of the hydrogen bond IR spectra in cinnamic acid crystals. Also suitable ab initio quantum chemical calculation result will be presented, in order to explain some aspects of the intensity distribution in the spectra.

For cinnamic acid crystals, four different-symmetry vibrational exciton states should exist, corresponding to a single quantum excitation of the proton stretching vibrations, in the four translationally non-equivalent hydrogen bonds of the unit cell. For the crystal, the *factor-group* is isomorphic with the  $C_{2h}$  point group. Therefore, in the limits of the strong exciton coupling model, only two allowed vibrational transitions in the IR should occur to the  $A_u$  and  $B_u$ -symmetry exciton states, generating two bands in the crystal spectra, each polarized parallel to one of the different identity periods of the lattice.

Initial analysis of the linear dichroic and the temperature effects, observed in the  $\nu_{\text{O-H}}$  band frequency range suggests that at least three component bands participate in formation of the  $\nu_{\text{O-H}}$  band in the crystalline spectra. This fact finds its explanation in the recently published papers, concerning the mechanisms of generation of centrosymmetric hydrogen bond dimer IR spectra, for the frequency range of the proton stretching vibration bands [20]. This general mechanism incorporates another sub-mechanism, depending on breaking of the conventional dipole selection rules, when exciting the totally symmetric proton stretching vibrations in such dimers. The totally symmetric proton vibrations in centrosymmetric dimers of hydrogen bonds become spectrally active in the IR via a vibronic promotion mechanism, which might be considered as a kind of 'reversion' of the familiar *Herzberg-Teller* mechanism [20]. It originally explained spectral properties in the UV of aromatic hydrocarbons (benzene) [34].

Single, isolated hydrogen bond dimers, formed in the gaseous phase, or in the  $\text{CCl}_4$  solution, exhibit two different subbands in their IR spectra, contributing to the  $\nu_{\text{X-H}}$  band, differing by their genesis [20]. The first sub-band, corresponding to the symmetry-allowed transition to the  $A_u$  excited state, should appear at the higher frequencies. The second sub-band, related to the symmetry-forbidden transition to the  $A_g$  excited state, appears at the lower frequencies, due to the vibronic activation mechanism. It 'borrows' its intensity from the allowed transition and it is generally of a lower intensity [20].

Spectral properties of model centrosymmetric hydrogen bond dimers satisfactorily explain the spectra of the majority of carboxylic acid crystals, with two centrosymmetric hydrogen bond dimers in a unit cell, when neglecting a weak inter-dimer exciton coupling between the non-equivalent dimers. In such a case, the crystal spectral properties fairly resemble spectral properties of 'oriented-gas', composed by these dimers. Such spectral behavior



seems to be a common property of carboxylic acid crystals [27,33]. In such cases, however, some slight, but measurable differences between the dichroic properties of the  $\nu_{\text{O-H}}$  band spectral branches, may appear [35,36].

In the case of a relatively strong vibrational exciton coupling between the dimers in each unit cell, polarization effects in the crystalline spectra should appear, corresponding to generation of four exciton vibrational states, originating directly from the two proton dimeric excited vibrational states. The cinnamic acid crystal spectral behavior seems to strictly correspond to the latest case. In our discussion, concerning the polarized IR spectra of cinnamic acid crystals, we will utilize the results of the recent theoretical, as well as experimental studies on the hydrogen bond dimeric systems, other carboxylic acid crystals included. Our consideration will start from the isotopic dilution effects in the crystalline spectra, which seem provide a key data for understanding the basic crystal spectral properties.

### 5.1. Isotopic dilution effects in the crystal spectra

As a result of the isotopic dilution the  $\nu_{\text{O-H}}$  band fine structure patterns in the crystalline spectra undergo a considerable simplification, generally resembling the band structure of the spectra, measured in  $\text{CCl}_4$  solution. In non-polar solvent solutions, the dominating forms of associates are centrosymmetric dimers of cinnamic acid. The observed similarity of the solution and of the isotopically diluted crystal spectra suggests that for the crystals just centrosymmetric hydrogen bond dimers are just the structural units, which are responsible for generation of the ‘residual’  $\nu_{\text{O-H}}$  bands. This statement may be supported by an initial analysis of the ‘residual’  $\nu_{\text{O-H}}$  band dichroic properties, which do not anymore exhibit the *Davydow-splitting* effect, ascribed to the exciton coupling between the translationally non-equivalent dimers from each unit cell. The ‘residual’  $\nu_{\text{O-H}}$  band shapes appeared to be highly independent from the crystalline face, accepted for an individual spectral experiment. These polarized bands exhibit the polarization effect of the ‘first kind’, corresponding to the geometrical factors in the experimental conditions. Therefore, the hydrogen bond lattice in an isotopically diluted crystal spectrally behaves as ‘oriented-gas’, composed with the randomly distributed in the lattice hydrogen bond dimers.

From the spectra it results that the isotopic dilution did not cause a fully random distribution of the hydrogen and of the deuterium bonds, in the lattice of cinnamic acid crystals. This latter constatation proves that some non-conventional, co-operative effects take place in such crystals, depending on a non-random distribution of protons and deuterons in the hydrogen bond lattice. These so-called H/D isotopic ‘self-organization’ effects were described only recently for crystals, with their lattices containing centrosymmetric, cyclic hydrogen bond dimers [22,25] and for another type of

crystals, with infinite chains of hydrogen bonds in their lattices [23,24]. In the case of cinnamic acid crystals, the isotopic dilution leads to a mixture of the ‘HH’ and of the ‘DD’-type dimers only, with a negligibly small concentration of the ‘HD’-type mixed dimers. The ‘HH’ and the ‘DD’ dimers contain two identical hydrogen isotope atoms in their hydrogen bonds. In turn, these symmetric dimers are fully randomly distributed in the crystal lattice. Such a partial disorder in the lattice is responsible for annihilation of some *Davydow-splitting* effects, in the spectra of isotopically diluted crystals. This conclusion can be derived when based on comparison of the all analyzed polarized crystalline spectra, measured in the frequency range of the  $\nu_{\text{O-H}}$  bands and of the ‘residual’  $\nu_{\text{O-H}}$  bands.

## 6. Model calculations of the ‘residual’ $\nu_{\text{O-H}}$ and $\nu_{\text{O-D}}$ band contours

### 6.1. Numerical reconstitution of the ‘residual’ $\nu_{\text{O-H}}$ and $\nu_{\text{O-D}}$ band contours

Model calculations, aiming to reconstitute the ‘residual’  $\nu_{\text{O-H}}$  and  $\nu_{\text{O-D}}$  band shapes on a theoretical way, were performed in the limits of the ‘strong-coupling’ model [6,7,17], for a centrosymmetric, cyclic hydrogen bond dimer. In terms of this model, the  $\nu_{\text{O-H}}$  and  $\nu_{\text{O-D}}$  band structures were treated as superposition of two component bands, corresponding to excitation of two kinds of the proton stretching vibrations, i.e. of the totally symmetric ‘in-phase’ and of the non-totally symmetric ‘out-of-phase’ vibrations. The first of the above-mentioned bands is of a lower frequency, in comparison with the frequency of the second band.

Within the ‘strong-coupling’ theory, the  $\nu_{\text{O-H}}$  band shape for a dimer, composed with two  $\text{O-H}\cdots\text{O}$  hydrogen bonds, basically depends on the following system of coupling parameters: (i) On the distortion parameter ‘ $b_{\text{H}}$ ’, and on (ii) the resonance interaction parameters ‘ $C_0$ ’ and ‘ $C_1$ ’ [6,7,17]. Each parameter has a precisely defined physical meaning: The ‘ $b_{\text{H}}$ ’ parameter describes the change in the equilibrium geometry for the low-energy hydrogen bond stretching vibrations, accompanied to the excitation of the high-frequency proton stretching vibrations  $\nu_{\text{O-H}}$ . The ‘ $C_0$ ’ and ‘ $C_1$ ’ parameters are responsible for mutual interactions between the hydrogen bonds in a dimer, in its vibrationally excited state. They denote subsequent expansion coefficients in the series, when developing the resonance interaction integral ‘ $C$ ’, with respect to the normal coordinates of the low frequency, hydrogen bond stretching vibrations  $\nu_{\text{O}\cdots\text{O}}$ :

$$C = C_0 + C_1 Q_1;$$

where  $Q_1$  represents the totally symmetric normal coordinate, for the low-frequency stretching vibration in the dimer. These parameters remain in a close relation with the intensity

distribution in the dimeric  $\nu_{\text{O-H}}$  band: The ' $b_{\text{H}}$ ' and ' $C_1$ ' parameters are directly connected with the dimeric  $\nu_{\text{O-H}}$  bandwidth. The ' $C_0$ ' parameter determines the splitting of the component bands of the dimeric spectrum, corresponding to excitation of the proton vibrational motions of different-symmetry [6,7,17]. In its original version, the 'strong-coupling' model predicts diminution of the distortion parameter value for deuterium bond systems, according to the relation:

$$b_{\text{H}} = \sqrt{2}b_{\text{D}}.$$

For the ' $C_0$ ' and ' $C_1$ ' resonance interaction parameters, the theory predicts the H/D isotopic effect, expressed by diminution by 1.0 to  $\sqrt{2}$  times of the parameter values.

The strong narrowing of the  $\nu_{\text{O-D}}$  bands in the spectra of cinnamic acid crystals is thus a result of an extremely strong coupling between vibrations in a dimer. It is expressed by a linear dependence of the resonance interaction integral ' $C$ ', for vibrationally excited hydrogen bonds in the dimer, upon the normal coordinate ' $Q_1$ ' of the low-frequency hydrogen bond vibration [17]. Our calculation results reproduce only some general properties of the analyzed bands. In the case of reconstitution of the 'residual'  $\nu_{\text{O-H}}$  bands it was necessary to take in to the account, with a relatively high statistical weight ' $F^-$ ', of the dimeric 'minus' sub-band, corresponding to the 'in-phase' proton vibrations, reproducing the longer-wave branches of the bands. The allowed transition participates in the band generation mechanism with the ' $F^+$ ' statistical weight factor. The model calculations have proved that the assumed centrosymmetric dimeric hydrogen bond model explains satisfactorily the basic spectral properties of the cinnamic acid isotopically diluted crystals.

A thorough analysis of the band shapes from Figs. 2–8 allows identifying of a local lowering of the  $\nu_{\text{O-H}}$  band contours, appearing at the range of 2700–2800  $\text{cm}^{-1}$ . These irregularities, resembling the so-called 'Evans holes', are most probably a manifestation of *Fermi resonance* mechanisms, acting in centrosymmetric hydrogen bond dimers. These anharmonic resonances most probably involve the proton stretching vibrations in the hydrogen bonds and the  $\delta_{\text{O-H}}$  proton 'in plane' bending vibrations, in their first overtone state [37]. Very similar spectral effects were observed recently, in the spectra of arylcarboxylic acid crystals [28,30]. On the other hand, no such effects were found in the spectra of arylacetic acid crystals [29] as well as in the spectra of aliphatic dicarboxylic acid crystals [27,33]. These all facts suggest that a vibronic coupling, involving the hydrogen bond protons in the dimers, with the  $\pi$ -electrons from aromatic ring systems, is responsible for an additional stabilization of the cinnamic acid dimers. This interaction seems responsible for strengthening of the anharmonic coupling between the two different proton normal vibrations.

Taking in to the account of the *Fermi resonance* in the 'strong-coupling' model calculations allowed obtaining a better similarity between the calculated  $\nu_{\text{O-H}}$  band contour

shape, when compared with the corresponding experimental spectrum of cinnamic acid crystal. A similar calculation method was utilized as for interpretation the IR spectra of benzoic acid crystals [28].

In Fig. 9 the model calculation results are being shown, aiming to quantitatively reconstitute 'residual'  $\nu_{\text{O-H}}$  band

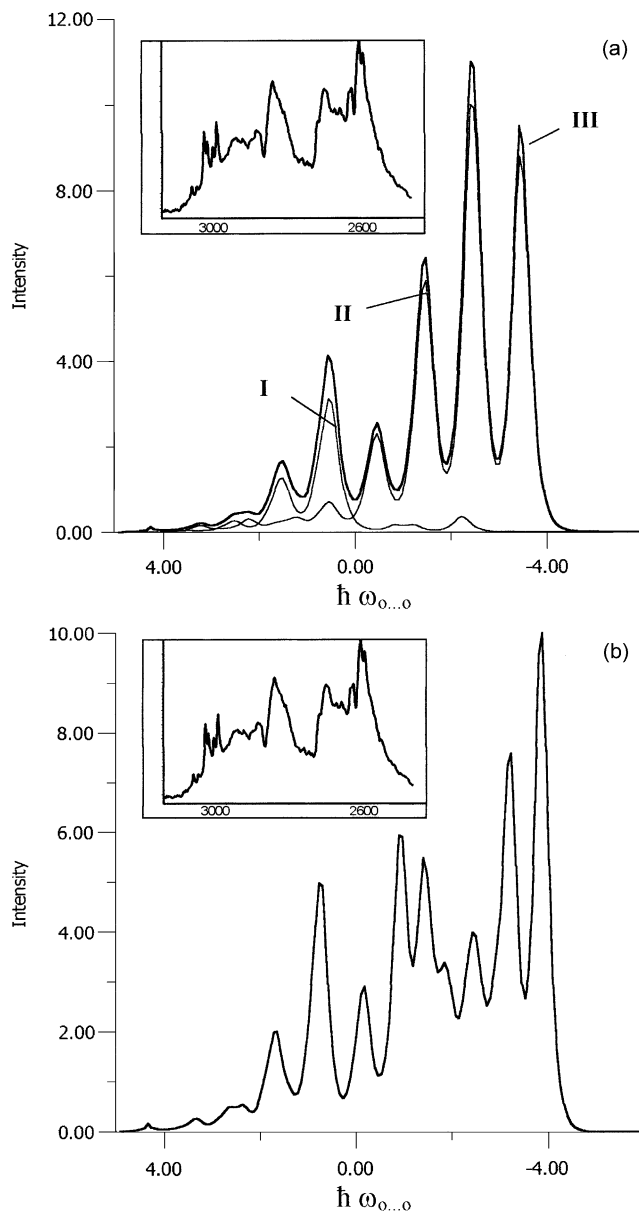


Fig. 9. Theoretical reconstitution of the most intense 'residual'  $\nu_{\text{O-H}}$  band component from the low-temperature spectra of isotopically diluted cinnamic acid crystals. (a) The band shape simulation in the limits of the 'strong-coupling' model: (I) The 'plus' dimeric band reconstituting the symmetry-allowed transition band, (II) the 'minus' dimeric band reproducing the forbidden transition band, (III) the superposition of the 'plus' and 'minus' bands taken with their statistical weight parameters  $F^+$  and  $F^-$ . The coupling parameter values:  $b_{\text{H}}=1.2$ ,  $C_0=1.4$ ,  $C_1=-0.3$ ,  $F^+=0.2$ ,  $F^-=1.0$ ,  $\Omega_{\text{O}...\text{O}}=90 \text{ cm}^{-1}$ . (b) The spectrum 'a' after introducing the *Fermi resonance* correction. Transition energies are given in the  $\nu_{\text{O}...\text{O}}$  hydrogen bond stretching vibration quantum units. Intensities are given in arbitrary units. The corresponding experimental spectrum is presented at the left upper edge of each sub-picture.

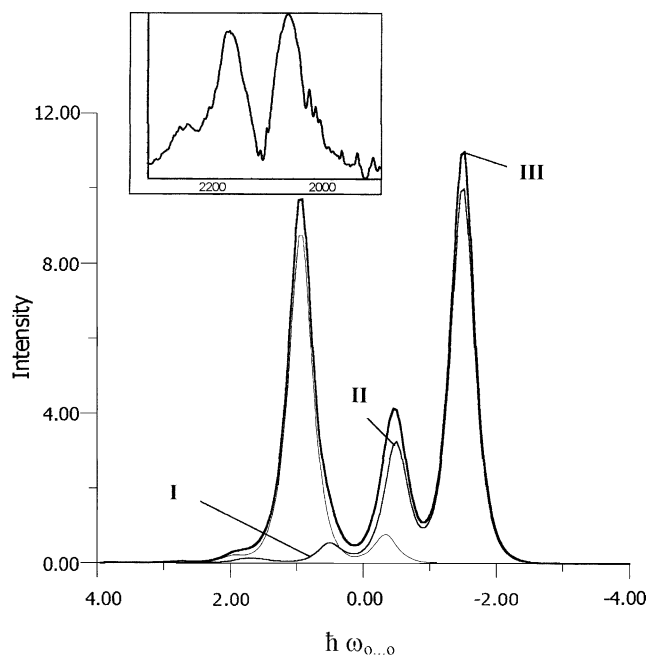


Fig. 10. Theoretical prediction of the most intense  $\nu_{\text{O-D}}$  band component from the low-temperature spectra of cinnamic acid crystals. (I) The 'plus' dimeric band, (II) the 'minus' dimeric band reproducing the forbidden transition band, (III) the superposition of the 'plus' and 'minus' bands taken with their statistical weight parameters  $F^+$  and  $F^-$ . The coupling parameter values:  $b_D=0.6$ ,  $C_0=1.0$ ,  $C_1=-0.2$ ,  $F^+=0.7$ ,  $F^-=1.0$ ,  $\Omega_{\text{O} \cdots \text{O}}=90 \text{ cm}^{-1}$ . The corresponding experimental spectrum is presented at the left upper edge of the picture.

contour shapes, from the spectra of isotopically diluted by deuterium cinnamic acid crystals. The model calculations were performed in the limits of the 'strong-coupling' model [6,7,17], in the centrosymmetric hydrogen bond dimer approximation, with taking in to the account of the *Fermi resonance* interactions in the dimer.

Quantitative reproduction of the  $\nu_{\text{O-D}}$  band contour shapes from the spectra of cinnamic acid crystals, isotopically diluted by hydrogen, is being presented in Fig. 10.

Based on the results of our model calculations and also accepting our interpretation of the generation mechanisms of the crystal spectra, the temperature effect may be explained, recorded in the frequency ranges of the  $\nu_{\text{O-H}}$  and the  $\nu_{\text{O-D}}$  bands. The intensity diminution of the longer-wave branch of each band, when temperature grows, is most probably connected with declining of the  $(\text{COOH})_2$  cycle average geometry from the low-temperature structure, towards a more symmetric one, due to large-amplitude low-energy vibrational motions.

## 6.2. The *ab initio* calculations

The intensity of the forbidden transition sub-band of the  $\nu_{\text{O-H}}$  band in the spectra of cinnamic acid crystal is extremely high. Very similar band properties were observed in the spectra of benzoic acid crystals [28]. On the other

hand, an extremely low intensity of the longer-wave branch of the  $\nu_{\text{O-H}}$  band was found in the spectra of phenylacetic acid crystals [29].

The theoretical model, proposed for explaining of the forbidden vibrational transition mechanism, attributes this phenomenon to electronic properties of hydrogen bonds [20]. One might expect that an extremely high relative intensity of the symmetry forbidden transition sub-band, representing the longer-wave branch of the  $\nu_{\text{O-H}}$  band, would be related to a considerably large excess electronic charge, grouped on the associated carboxyl groups in the cinnamic acid dimers. Very similar correlation between the longer-wave  $\nu_{\text{O-H}}$  band branch intensities and the excess electronic charge on the carboxyl groups was recently discussed for the IR spectra of 1-naphthoic and 2-naphthoic acid crystals [30]. These facts suggest that the electronic charge can be partially withdrawn from the conjugated  $\pi$ -bond systems, by the dimeric hydrogen bonds, however, the magnitude of this effect is a property of an individual carboxylic acid molecule electronic structure. Following this idea one may expect that the charge withdrawal is most effective in the case of the cinnamic acid dimers and it is less effective for the phenylacetic acid dimers.

To explain the phenomenon of the extremely high intensity of the forbidden transition sub-band, we performed the *ab initio* calculations of the excess electronic charge, on the hydrogen-bonded carboxyl groups of the cinnamic, benzoic and phenylacetic acid dimers.

Carboxyl groups effectively withdraw electronic charge from aromatic rings, or from more complex conjugated  $\pi$ -bond systems. For the hydrogen bonded dimeric system studies, this charge withdrawal is expected to be strongest, when the carboxyl groups are directly attached to a  $\pi$ -appropriate calculations were performed using the GAUSSIAN 98 series of programs [38] at the SCF (SCF—Self Consistent Field) and at the DFT-B3LYP (DFT—Density Functional Theory) level, with the 6-311G basis. A full optimization of the dimer geometry was assumed. Our calculations have shown that in the case of cinnamic acid, the carboxyl group most effectively withdrew electrons from the  $\pi$ -electronic styryl substituent system, in comparison with the benzoic acid and the phenylacetic acid case. These effects find its illustration in the calculated *Mulliken* charges, concerning the carboxyl group and the naphthyl ring atoms. At the SCF level, for cinnamic acid an excessive charge of  $-0.0077$  elementary electron charge has been estimated, when for benzoic acid the corresponding value was equal to  $+0.0199$  and for phenylacetic acid the corresponding value was equal to  $+0.0118$ .

At the DFT-B3LYP level the corresponding values were equal to  $-0.0375$ ,  $-0.0182$  and  $+0.0111$ , respectively. These latest calculations took in to the account electron correlations. Therefore, they should be considered as the more reliable ones.

When the electron charge from the aromatic ring is strongly shifted towards carboxyl group, vibronic coupling

mechanisms between the proton stretching vibrations and the hydrogen bond electrons, coupled with the electrons of aromatic rings, is strengthened. The enlarged electronic charge on the carboxyl group should be responsible for an increase of the hydrogen bond electronic polarization magnitudes, affected by the vibrating protons. This effect should result in an enhancement of the *Herzberg-Teller*-type vibronic coupling in the hydrogen bonds, involving the protons and the hydrogen bond electrons. In this case a stronger coupling can influence a more effective promotion mechanisms of the forbidden transitions in the IR, as the vibrational selection rule breaking mechanism is considered a reversion of the familiar *Herzberg-Teller* mechanism, explaining UV–Vis spectra of aromatic molecules [20]. This conclusion is also based on a general theory of vibrational transitions, which sees the source of IR band intensities in fine vibronic couplings in molecules. Thus, the selection rule breaking effect is expected to be stronger for the stronger electron withdrawal case, i.e. for cinnamic acid crystal. In such a way, different relative intensities of the longer-wave branches of the  $\nu_{\text{O-H}}$  and  $\nu_{\text{O-D}}$  bands may result for the spectra of the two crystalline systems. Therefore, in the spectra of phenylacetic acid, the forbidden transition effect is considered the weakest one, as the relative longer-wave  $\nu_{\text{O-H}}$  band branch intensity is ca. 5 times lower, when compared with the cinnamic acid crystal spectrum [30].

The above listed results, confronted with the cinnamic acid crystal spectra, suggest that the source of the extremely high intensity of the forbidden, longer-wave  $\nu_{\text{O-H}}$  band branch is a highly effective vibronic mechanism of the vibrational selection rule breaking in the IR [20]. This property correlates with the high excessive electronic population on the carboxyl groups of cinnamic acid dimers, when compared with the calculated corresponding values, found for the benzoic and the phenylacetic acid dimers.

The extremely low excess electronic charge, on the carboxyl groups of phenylacetic acid dimers, correlates with a very low intensity of the forbidden transition band, in the longer-wave branch of the  $\nu_{\text{O-H}}$  band, in the IR spectra of phenylacetic acid crystals. It means that the methylene groups are responsible for an effective isolation between the hydrogen bonds and the  $\pi$ -electronic systems, considerably weakening the forbidden vibrational transition mechanisms, for centrosymmetric hydrogen bond dimers of phenylacetic acid. At this point it seems worth to admit that in the spectra of styrylacetic acid crystals the longer-wave branch of the  $\nu_{\text{O-H}}$  band is also of a very low intensity [39].

## 7. Conclusion

The cinnamic crystal IR spectra investigation results, presented in this paper, allowed to identify most completely the nature of vibrational transitions, occurring in the hydrogen bond system, responsible for the generation of the  $\nu_{\text{O-H}}$  and  $\nu_{\text{O-D}}$  band fine structure pattern.

The complementary studies of the polarization, of the temperature and of the H/D isotopic effects, as well as of isotopic dilution effects in the crystal spectra, confronted with the model calculations, allowed ascribing these effects to a centrosymmetric hydrogen (or deuterium) bond dimer, as a proper model system. Such a dimer system is the source of the basic spectral properties of cinnamic acid crystals, determining the basic, two-branch structure of the analyzed bands. Exciton interactions, involving hydrogen bonds of the adjacent dimers in a unit cell, are responsible for generation of the secondary effects, mainly for appearance of doublet structures in  $\nu_{\text{O-H}}$  and  $\nu_{\text{O-D}}$  bands, due to the *Davydow-coupling* mechanisms.

Our studies have provided data, confirming the H/D ‘self-organization’ process scheme, for the hydrogen bond lattices of isotopically diluted cinnamic acid crystals. In the case of high deuterium exchange rates in cinnamic acid crystals, the remaining protons of a partially deuterated sample are grouped together in the symmetric ‘HH’-type dimers. In turn, the isotopic dilution effects in the spectra have provided data, crucial for understanding of the  $\nu_{\text{O-H}}$  and  $\nu_{\text{O-D}}$  band fine structure generation mechanisms, as selected *Davydow-coupling* effects in the crystal spectra vanish. Such decoupling of the hydrogen bonds noticeably simplified the spectrum fine structure patterns, facilitating further theoretical treatment of the problem.

The H/D ‘self-organization’ process may occur thanks to the easy-polarizable  $\pi$ -electron structure of cinnamic acid molecules. This molecular electronic property facilitates effective vibronic couplings between the vibrating protons and the electrons, in the hydrogen bond dimeric systems of the associated cinnamic acid molecules, which is the source of the H/D isotopic ‘self-organization’ processes in the crystals [25]. The electronic structure of cinnamic acid molecules is also the basic source of other non-conventional spectral effects, depending on breaking of vibrational dipole selection rules, for centrosymmetric hydrogen bond dimers formed in associated carboxyl groups. A very high intensity of the forbidden transition band, forming the longer-wave branch of the  $\nu_{\text{O-H}}$  band, is a result of a strong vibronic coupling, involving the hydrogen bond dimers and the  $\pi$ -electrons of the styryl substituent.

Very similar spectral behavior was also observed in the polarized IR spectra of 3-methylcinnamic acid crystals [39].

## References

- [1] G.C. Pimentel, A.L. McClellan, *The Hydrogen Bond*, W.H. Freeman, San Francisco, 1960.
- [2] P. Schuster, G. Zundel, C. Sandorfy (Eds.), *The Hydrogen Bond, Recent Developments in the Theory and Experiment*, Parts I, II and III, North-Holland, Amsterdam, 1976.
- [3] G.L. Hofacker, Y. Marechal, M.A. Ratner, The dynamical aspects of hydrogen bonds, in: P. Schuster, G. Zundel, C. Sandorfy (Eds.), *The Hydrogen Bond, Recent Developments in Theory and Experiment*, Part I, North-Holland, Amsterdam, 1976, p. 295.



- [4] P. Schuster, W. Mikenda (Eds.), *Hydrogen Bond Research*, Monatshefte für Chemie, Chemical Monthly, 130/No. 8, Springer, Wien, New York, 1999.
- [5] D. Hadzi (Ed.), *Theoretical Treatments of Hydrogen Bonding*, Wiley, New York, 1997.
- [6] A. Witkowski, J. Chem. Phys. 47 (1967) 3645.
- [7] Y. Marechal, A. Witkowski, J. Chem. Phys. 48 (1968) 3697.
- [8] S.F. Fisher, G.L. Hofacker, M.A. Ratner, J. Chem. Phys. 52 (1970) 1934.
- [9] O. Henri-Rousseau, P. Blaise, The infrared density of weak hydrogen bonds within the linear response theory, in: I. Prigogine, S.A. Rice (Eds.), *Advances in Chemical Physics* 103, Wiley, 1998.
- [10] D. Chamma, O. Henri-Rousseau, Chem. Phys. 248 (1999) 53.
- [11] D. Chamma, O. Henri-Rousseau, Chem. Phys. 248 (1999) 71.
- [12] D. Chamma, O. Henri-Rousseau, Chem. Phys. 248 (1999) 91.
- [13] J.L. Leviel, Y. Marechal, J. Chem. Phys. 54 (1971) 1104.
- [14] J. Bournay, Y. Marechal, J. Chem. Phys. 55 (1971) 1230.
- [15] P. Excoffon, Y. Marechal, Spectrochim. Acta Part A 28 (1972) 269.
- [16] M.J. Wójcik, Int. J. Quantum Chem. 10 (1976) 747.
- [17] H.T. Flakus, Chem. Phys. 62 (1981) 103.
- [18] H.T. Flakus, A. Bryk, J. Mol. Struct. 372 (1995) 215.
- [19] H.T. Flakus, A. Bryk, J. Mol. Struct. 372 (1995) 229.
- [20] H.T. Flakus, J. Mol. Struct. (Theochem) 187 (1989) 35.
- [21] H.T. Flakus, A. Machelska, J. Mol. Struct. 447 (1998) 97.
- [22] H.T. Flakus, A. Bańczyk, J. Mol. Struct. 476 (1999) 57.
- [23] H.T. Flakus, A. Tyl, P.G. Jones, Spectrochim. Acta A 58 (2002) 299–310.
- [24] H.T. Flakus, A. Machelska, Spectrochim. Acta A 58 (2002) 555–568.
- [25] H.T. Flakus, J. Mol. Struct. 646 (2003) 15–23.
- [26] H.T. Flakus, J. Mol. Struct. (Theochem) 285 (1993) 281.
- [27] H.T. Flakus, A. Miros, J. Mol. Struct. 484 (1999) 103.
- [28] H.T. Flakus, M. Chełmecki, Spectrochim. Acta A 58 (2001) 179–196.
- [29] H.T. Flakus, M. Chełmecki, Spectrochim. Acta A 58 (2002) 1867–1880.
- [30] H.T. Flakus, M. Chełmecki, J. Mol. Struct. 659 (2003) 103–117.
- [31] H.T. Flakus, M. Chełmecki, Polarization IR spectra of the hydrogen bond in 1-naphthylacetic and 2-naphthylacetic acid crystals, J. Mol. Struct. 705 (2004) 81–89.
- [32] R.F. Bryan, D.P. Freyberg, J.C.S. Perkin II, (1975) 1835.
- [33] H.T. Flakus, A. Miros, Spectrochim. Acta A 57 (2001) 2391–2401.
- [34] G. Fisher, *Vibronic Coupling*, Academic Press, London, 1984.
- [35] G. Auvert, Y. Marechal, Chem. Phys. 40 (1979) 51.
- [36] G. Auvert, Y. Marechal, Chem. Phys. 40 (1979) 61.
- [37] A. Witkowski, M.J. Wójcik, Chem. Phys. 1 (1973) 9.
- [38] M.J. Frisch, G.W. Trucks, H.B. Schlegel, G.E. Scuseria, M.A. Robb, J.R. Cheseman, V.G. Zakrzewski, J.A. Montgomery, R.E. Stratmann, J.C. Burant, S. Dappich, J.M. Millam, A.D. Daniels, K.N. Kudin, M.C. Strain, O. Farkas, J. Tomasi, V. Barone, M. Cossi, R. Cammi, B. Mennucci, C. Pomelli, C. Adamo, S. Clifford, J. Ochterski, G.A. Peterson, P.Y. Ayala, Q. Cui, K. Morokuma, D.K. Malick, A.D. Rabuck, K. Raghavachari, J.B. Foresman, J. Cioslowski, J.V. Ortiz, B.B. Stefanov, G. Liu, A. Liashenko, P. Piskorz, I. Komaromi, R. Gomperts, R.L. Martin, D.J. Fox, T. Keith, M.A. Al-Laham, C.Y. Peng, A. Nanayakkara, C. Gonzalez, M. Challacombe, P.M.W. Gill, B.G. Johnson, W. Chen, M.W. Wong, J.L. Andres, M. Head-Gordon, E.S. Replogle, J.A. Pople, GAUSSIAN 98 (Revision A.1), Gaussian, Inc., Pittsburgh PA, 1998.
- [39] H.T. Flakus, M. Jabłońska, non published results, in preparation.